Journal of Alloys and Compounds 493 (2010) 517–521

Contents lists available at ScienceDirect

Journal of Alloys and Compounds

journal homepage: www.elsevier.com/locate/jallcom

Fabrication and stability of the $Ca_{1-x}CuO_2$ chain structure during high-pressure and high-temperature sintering

X.M. Qin[a,b,*], W.J. Mai[b], J.M. Li[a], F.Y. Li[b], C.Q. Jin[b]

[a] Shanghai Normal University, Shanghai 200234, PR China
[b] Institute of Physics, Beijing High Pressure Research Center, Chinese Academy of Sciences, P.O. Box 603, Beijing 100080, PR China

ARTICLE INFO

Article history:
Received 20 May 2009
Received in revised form
19 December 2009
Accepted 26 December 2009
Available online 4 January 2010

Keywords:
High temperature
High pressure
High oxygen pressure
$Ca_{1-x}CuO_2$
Edge-sharing CuO_2 chains

ABSTRACT

$Ca_{1-x}CuO_2$ contains an infinite one-dimensional edge-sharing $[CuO_2]$ chain and is readily fabricated by a solid-state reaction in a moderate oxygen atmosphere (10–12 bar). High-temperature (890–1170 °C) and high-pressure (3.0–5.0 GPa) sintering was used to study the stability of the $Ca_{1-x}CuO_2$ samples. We found that the $Ca_{1-x}CuO_2$ chain structure remained stable at high temperature, high pressure and high oxygen pressure. However, we found that the stoichiometry of the $Ca_{1-x}CuO_2$ compound is modified after high-pressure sintering, suggesting that high-pressure sintering may increase the calcium content of the $Ca_{1-x}CuO_2$ chain structure.

1. Introduction

The most common non-copper metal elements in high-T_c superconductors (HTSC's) are alkaline earth metals such as Ca, Sr or Ba. To discover new HTSC's of simple composition and to understand the fundamental crystal chemistry of copper oxide superconductors it is very important to study AO–CuO binary oxide systems [1]. CaO–CuO compounds are composed of the very basic HTSC core agent, which builds up a so-called infinite layer unit $[CaCuO_2]$ of a homologous HTSC series.

Commonly encountered structures in the CaO–CuO system are the well-known corner-sharing chain compound Ca_2CuO_3 [2], the ladder compound $CaCu_2O_3$ [3], the infinite layer compound $CaCuO_2$ [4] and the edge-sharing chain structure compound $Ca_{1-x}CuO_2$ ($0.80 \le x \le 0.85$) [5,6]. Their simple compositions and structural features allow the development of theories that may be used to investigate the superexchange interaction J of Cu–O by considering different types of bonding and different angle geometries. These theories may also allow for the detection of novel superconductivity. Siegrist et al. reported interesting results for a (Ca,Sr)O–CuO binary system [5,7]. They reported the discovery of superconductivity for the $[Cu_2O_3]$ ladder compound $(Sr,Ca)_{14}Cu_{24}O_{41}$ under high pressure [8] as well as in the double-chain compound $Pr_2Ba_4Cu_7O_{15-\delta}$ [9] implying that between the 2-D $[CuO_2]$ plane and the 1-D $[CuO_2]$ chain a bonanza of physics and materials exists. CaO–CuO compounds are also important precursors for the high-pressure synthesis of novel superconducting homologous series compounds such as $CuBa_2Ca_{n-1}Cu_nO_{2n+2+x}$, i.e. Cu-12$(n-1)n$ [10,11] of which the $n = 4$ (Cu-1234) compound has a 117 K superconductive transition.

Two types of infinite one-dimensional copper–oxygen chains exist and they consist of CuO_4 squares in the CaO–CuO system. One type is a corner-sharing chain as in Ca_2CuO_3 and the other is an edge-sharing chain as in $Ca_{1-x}CuO_2$ and this is shown in Fig. 1(a). Ca_2CuO_3 is a chemically stoichiometric compound with an average Cu^{2+} valence while $Ca_{1-x}CuO_2$ is hole doped due to calcium site vacancies. These two compounds differ in chain geometry as well. The different copper–oxygen chains result in many different physical properties and this is due to the exchange interaction J between Cu^{2+} ions in the corner-sharing chain being larger because of the 180° Cu–O–Cu superexchange interaction while J for the edge-sharing squares is greatly weakened because of the near 90° Cu–O–Cu superexchange interaction [12]. Chains of corner-sharing squares are also found in many HTSCs such as in $YBa_2Cu_3O_{7-\delta}$ [13]. We recently performed joint high-pressure studies using synchrotron radiation and investigated *in situ* electrical properties of the Ca_2CuO_3 compound and observed that although the crystal structure of Ca_2CuO_3 is quite stable under pressures up to 30 GPa a very interesting evolution of the electronic structure may take

* Corresponding author at: Shanghai Normal University, Shanghai 200234, PR China. Tel.: +86 21 64322726.
E-mail addresses: xmqin@shnu.edu.cn, xiaomei280@msn.com (X.M. Qin).

0925-8388/$ – see front matter © 2010 Elsevier B.V. All rights reserved.
doi:10.1016/j.jallcom.2009.12.147

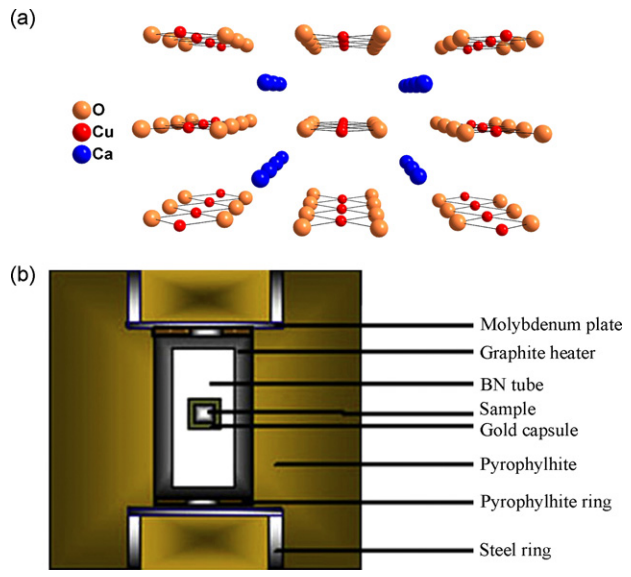

Fig. 1. (a) $Ca_{1-x}CuO_2$ as viewed along the edge-sharing chains. (b) Schematic map of the cell assembly for high-pressure synthesis.

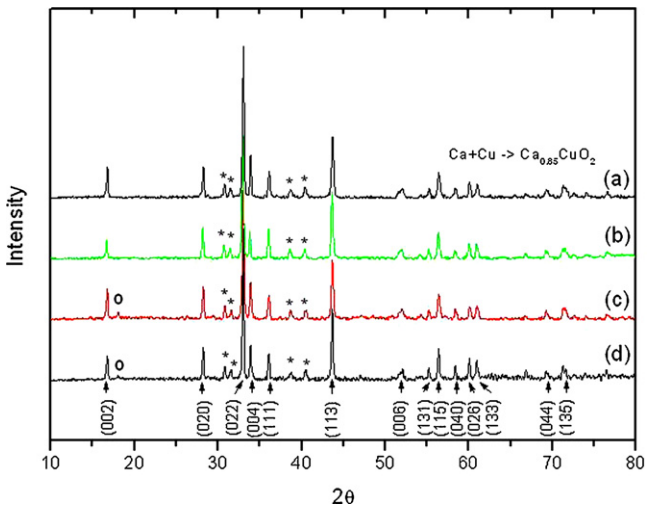

Fig. 2. XRD patterns of $Ca_{1-x}CuO_2$. Peaks marked with "*" are assigned to the incommensurate superstructure while the peak marked with "o" is assigned to $Ca(OH)_2$ (similar marks are used in the following figures): (a) XRD pattern of $Ca_{0.85}CuO_2$ as synthesized from CaO and CuO. (b) XRD pattern of $Ca_{0.85}CuO_2$ as synthesized from Ca_2CuO_3 and CuO. (c) XRD pattern of $CaCuO_2$ as synthesized from CaO and CuO. (d) XRD pattern of $CaCuO_2$ as synthesized from Ca_2CuO_3 and CuO.

place [14]. The $Ca_{1-x}CuO_2$ compound that consists of simple edge-sharing chains has been of interest since its discovery by Roth et al. in the 1990s [5,15]. The coexistence of antiferromagnetic long-range order and a spin-singlet state in low-dimensional cupric oxide $Ca_{1-x}CuO_2$ compounds are thought to be related to their high-T_c superconductivity [16]. The chain structure of $Ca_{1-x}CuO_2$ is observed as a low-temperature phase and is related to the $NaCuO_2$-type parent structure. It has an orthorhombic substructure with lattice parameters of $a = 0.2807$ nm, $b = 0.6351$ nm and $c = 1.0597$ nm [15]. Edge-sharing chains made from $[CuO_4]$ squares are situated in planes that are parallel to the (0 1 0) plane and the chains are also parallel with the Ca channels in the same a-axis direction. For the stoichiometric compound, the composition of the $Ca_{1-x}CuO_2$ crystal would be $CaCuO_2$ but during the study of pure samples obtained in low oxygen pressure it was found that only 0.8–0.85 of all calcium sites were occupied and thus periodic vacant sites were present [6,15,17–19]. These vacancies resulted in some magnetic Cu^{2+} ions ($S = 1/2$) becoming nonmagnetic Cu^{3+} ions ($S = 0$) and this had a great impact on their crystalline magnetic property [20,21].

High-pressure synthesis is a very important route to produce HTSCs and other related compounds [22,23]. High pressure during synthesis thermodynamically stabilizes close packed perovskite structures as has been very well demonstrated in geophysical studies of the Earth Mantle structure decades ago. Therefore, high pressure has been successfully employed to synthesize a series of novel HTSCs [24,25]. For example, in the simple A–Cu–O system, Smith et al. obtained a n-type infinite layer superconductor $Sr_{1-x}Nd_xCuO_2$ with a T_c of ≈40 K using high-pressure synthesis [26]. High pressure also has a great impact on material properties. The highest recorded T_c was obtained for $HgBa_2Ca_2Cu_3O_8$ under high-pressure conditions [27].

In this paper we report a synthesis of the infinite chain structure compound $Ca_{1-x}CuO_2$ ($x = 0, 0.15$) using different starting materials and investigate its stability using high-temperature, high-pressure and high oxygen pressure treatment.

2. Experimental

$Ca_{1-x}CuO_2$ samples ($x = 0, 0.15$) were prepared by a standard solid-state reaction method. Highly pure CaO and CuO were weighed and mixed in proportions of 0.85:1 and 1:1. The mixtures were then ground with an agate mortar for 0.5–1 h. The thoroughly mixed powder was pressed into pellets, wrapped in Ag foil and then sealed with a specific amount of Ag_2O in an evacuated quartz tube. The material was calcined in a low oxygen pressure atmosphere (10–12 bar and generated by the high-temperature decomposition of Ag_2O) at 750 °C for 24 h followed by a furnace quench. Alternatively, Ca_2CuO_3 and CuO may be used as starting materials to prepare $Ca_{0.85}CuO_2$ and $CaCuO_2$ compounds using a similar synthetic procedure described previously.

Singh suggested that the $Ca_{1-x}CuO_2$ phase has a lower density than the $[CaCuO_2]$ infinite layer structure and that it might be less stable under high pressure. $Ca_{1-x}CuO_2$ ($x = 0$) should be more susceptible to pressure than $Ca_{1-x}CuO_2$ ($x = 0.15$) and therefore a study of $Ca_{1-x}CuO_2$ ($x = 0$) under high pressure would provide insights into the stability of $Ca_{1-x}CuO_2$.

The stability of $Ca_{1-x}CuO_2$ ($x = 0$) compounds with regard to pressure, temperature and partial oxygen pressure was, therefore, investigated under the following three conditions:

(1) At a pressure of 4.5 GPa, $Ca_{1-x}CuO_2$ samples were treated at different temperatures of 890, 960, 1030, 1100, 1130 and 1170 °C for 20 min.
(2) At a temperature of 1030 °C, $Ca_{1-x}CuO_2$ samples were treated at different pressures of 3, 3.5, 4, 4.5 and 5 GPa for 20 min.
(3) With Ag_2O acting as an oxygen source, the $CaCuO_2$ samples were mixed with Ag_2O in molar proportions of ($m = Ag_2O{:}CaCuO_2 = 0.2, 0.4, 0.6, 0.8$ and 1.0). The mixtures were then treated at a pressure of 4.5 GPa and a temperature of 1030 °C for 20 min to investigate the stability of $CaCuO_2$ under high oxygen pressure conditions.

All these high-pressure treatments were carried out using a cubic anvil type high-pressure machine. As shown in Fig. 1 (b), the sample pellet was tightly packed into a gold capsule to avoid contamination and placed into a BN tube. This was then inserted into a graphite sleeve which acted as an electric heater. The sample was subjected to high-pressure treatment using pyrophyllite as a pressure-transmitting medium at the desired temperature and pressure for specific time, and this was followed by high-temperature and high-pressure quenching. The pressure was calibrated using the phase transition points of Bi(I–II at 2.55 GPa, II–III at 3.67 GPa), Tl(I–II at 2 GPa) and Ba(III–IV at 7.7 GPa) metals. The temperature was obtained from the relationship between heating power and temperature in the cell, as determined before the experiments. Product structure and composition was characterized by powder X-ray diffraction (XRD) using a rotating anode target type X-ray diffractometer (Rigaku X-ray diffractometer) and a scanning electron microscope (SEM) with EDX.

3. Results and discussion

Fig. 2 shows a powder XRD of the obtained $Ca_{0.85}CuO_2$ and $CaCuO_2$ samples. From Fig. 2a and b it is clear that the $Ca_{0.85}CuO_2$ samples are pure with no evidence of excess CaO or CuO or other phases as all the peaks belong to the $Ca_{0.85}CuO_2$ chain structure. The reflections marked by "*" originate from the commensurate and incommensurate ordering of Ca^{2+} cations in the

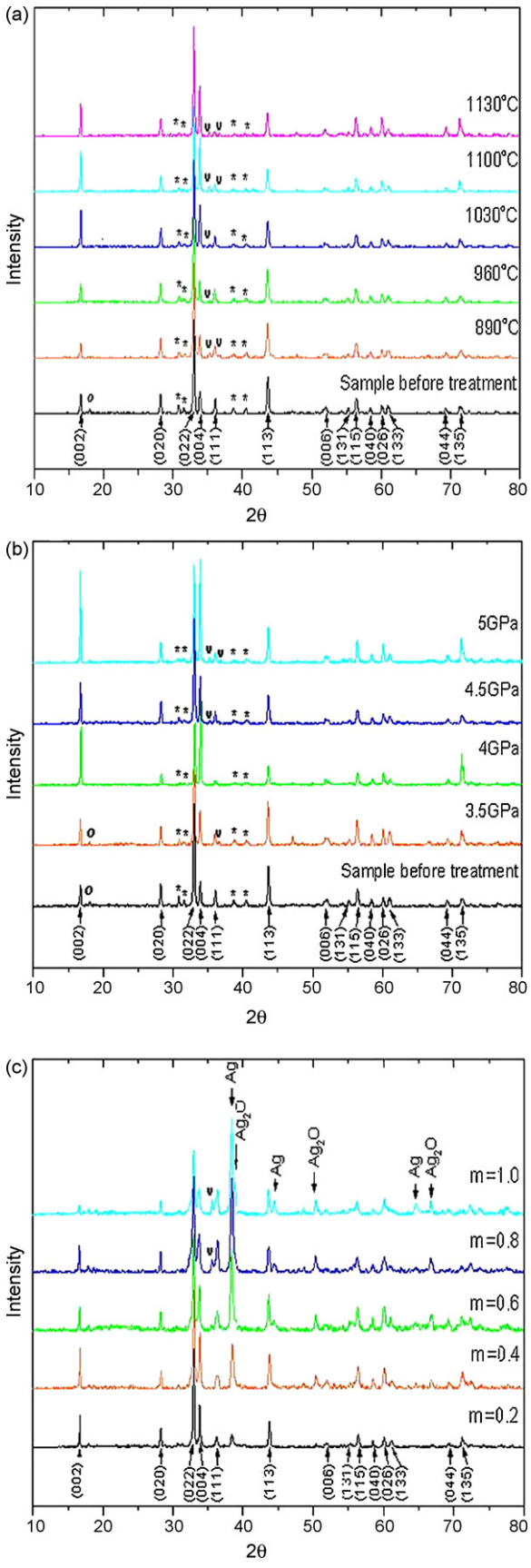

Fig. 3. XRD patterns of $CaCuO_2$ after different treatments. Peaks marked with "v" are reflections that appear after treatment (similar marks are used in the following figures): (a) XRD patterns of $CaCuO_2$ after different temperature treatments at a fixed pressure. (b) XRD patterns of $CaCuO_2$ after different pressure treatments at a fixed temperature. (c) XRD patterns of $CaCuO_2$ after oxygen pressure treatments at a fixed pressure and temperature with variable amounts of oxidizer.

Table 1
Starting materials, proportion of Ca:Cu in starting materials and product composition relationships for sintering experiments in a moderate oxygen environment.

Starting materials	Proportion of Ca:Cu	
	0.85:1	1:1
$Ca_2CuO_3 + CuO$	Pure $Ca_{1-x}CuO_2$	$Ca_{1-x}CuO_2 + Ca(OH)_2$
$CaO + CuO$	Pure $Ca_{1-x}CuO_2$	$Ca_{1-x}CuO_2 + Ca(OH)_2$

channels and this has also been reported by another group [18].

On the other hand, the $CaCuO_2$ samples are always composed of a $Ca_{0.85}CuO_2$ chain phase and excess calcium impurity. Their XRD spectra differ from that of $Ca_{0.85}CuO_2$ by the additional reflection marked as "o", which is the second strongest reflection of the $Ca(OH)_2$ impurity phase. The strongest reflection overlaps with the (0 0 4) reflection of $CaCuO_2$ and is thus indistinguishable. $Ca(OH)_2$ is present because Ca is in excess in the 1:1 mixture [6,15,17–19]. Reflections marked with "*" are also seen in Fig. 2c and d and no impurities besides $Ca(OH)_2$ were identified.

Although the $Ca_{1-x}CuO_2$ ($x = 0$, 0.15) samples were prepared using the aforementioned starting materials ($CaO + CuO$ or $Ca_2CuO_3 + CuO$), the final powder XRD patterns of the products are the same as those shown in Fig. 2. Therefore, it seems that the $Ca_{1-x}CuO_2$ structure is not strongly related to the starting materials as long as a moderate oxygen pressure is provided that facilitates the phase formation of $Ca_{1-x}CuO_2$. This conclusion was confirmed by related experiments. For example, after calcination of CaO and CuO in air we obtained a mixture of Ca_2CuO_3 and excess CaO or CuO and when using oxygen pressures as low as 10–12 bar a stable $Ca_{1-x}CuO_2$ was obtained. This indicates that an oxygen atmosphere is necessary to obtain a $Ca_{1-x}CuO_2$ chain structure using the solid-state reaction. This may be due to the low decomposition temperature of $Ca_{1-x}CuO_2$ in air as it can easily transform into $Ca_2CuO_3 + CaO$ at 755 ± 5 °C and this temperature increases to 835 ± 5 °C in flowing oxygen ($P(O_2) = 1$ bar) [6]. The temperature used during synthesis in our experiment was 750 °C so that a moderate oxygen environment was indispensable. The formal copper valence (FCV) in $Ca_{0.85}CuO_2$ is 2.4 and, therefore, thermodynamically this phase is favored at higher oxygen pressures. Table 1 lists the starting materials, proportion of Ca:Cu and product composition relationships when sintering in a moderate oxygen environment.

During the investigation of $CaCuO_2$ stability, we found that the chain structure is quite stable under high pressure and high temperature. Fig. 3a shows the powder XRD of a series of $CaCuO_2$ samples treated at a pressure of 4.5 GPa and at various temperatures from 890 to 1130 °C. We observed that $CaCuO_2$ melted and decomposed at temperatures higher than 1130 °C. The phase stability of $CaCuO_2$ at 1030 °C was maintained from 3.5 to 5 GPa as shown in Fig. 3b. It melted at 3 GPa because the melting temperature is less at lower pressure. Since the $Ca_{1-x}CuO_2$ compounds are hole doped in comparison to the Cu 2+ parent valence, we further investigated the phase stability of $CaCuO_2$ under high oxygen pressure. Fig. 3c shows the powder XRD patterns of $CaCuO_2$ treated at 4.5 GPa, 1030 °C and at high oxygen pressure with various amounts of oxidizer m (the molar ratio of Ag_2O:$CaCuO_2$). The oxygen originates from the decomposition of Ag_2O. It is clear that with an increase in the amount of Ag_2O the reflections of Ag and Ag_2O become stronger and that the $Ca_{1-x}CuO_2$ chain structure remains stable under high oxygen pressure. After high-temperature and high-pressure sinter-

ing, reflections such as (0 0 2) and (0 0 4) become relatively strong and this may be due to a change in the preferred orientation. The (1 1 1) reflection becomes wider, lower and even triplet (new peaks are marked with "v") after high-temperature and high-pressure treatments for an unknown reason.

This result is consistent with the report of Hayashi et al. who succeeded in preparing *Y*-substituted samples of $(Ca_{1-y}Y_y)_{1-x}CuO_2 (0 \le y \le 0.5, x = 0.2)$ using 215 bar of oxygen pressure [11]. These results indicate that the $Ca_{1-x}CuO_2$ structure is preferred in an oxygen atmosphere. This means that once formed, the $Ca_{1-x}CuO_2$ chain structure will remain stable in an oxygen environment. It tends to separate from complex ternary or quaternary cuprates at high $P(O_2)$ and thus the structure of any HTSC will be destabilized thereby hindering formation of the desired HTSC phase in a stoichiometric ratio.

It is interesting to note that after high-pressure treatment the samples show a dramatic decrease in the amount of $Ca(OH)_2$ impurity. The XRD patterns shown in Fig. 3 reveal that reflections due to $Ca(OH)_2$ no longer exist in the spectra of the high-pressure annealed samples and no other phases containing Ca were found. Moreover, the reflections that originate from the commensurate and incommensurate ordering of Ca^{2+} cations become much weaker. Materials after high-pressure treatment would usually be far more compact and vacancies in the structure would probably be occupied with corresponding atoms. We therefore infer that the excessive Ca that was supplied as $Ca(OH)_2$ in the second phase might react with $Ca_{1-x}CuO_2$ at high pressure and high temperature resulting in the migration of calcium in the $Ca(OH)_2$ phase to the Ca site voids in the non-stoichiometric $Ca_{1-x}CuO_2$ chain structure. This consequently leads to a change in Cu valency for the $Ca_{1-x}CuO_2$ structure and results in an interesting property evolution, especially in terms of magnetism.

Fig. 4 shows SEM micrographs of typical $Ca_{1-x}CuO_2$ samples. Fig. 4a shows that $Ca_{0.85}CuO_2$ contains fine crystal grains and that their distribution is homogenous with an average grain size of several μm. On the other hand, Fig. 4b shows a SEM micrograph of a pristine $CaCuO_2$ sample and reveals that in addition to small crystal grains ("A") with a composition close to that found in pristine $Ca_{0.85}CuO_2$, several big flat-like crystal grains ("B") of tens of μm in size are also present. The EDX analysis indicated that the B-region is dominated by Ca, which most likely corresponds to $Ca(OH)_2$ as detected by powder XRD and this is shown in Fig. 2c. Fig. 4c is a typical SEM of a high-pressure treated $CaCuO_2$ sample and shows a compacted polycrystal. The overall atomic ratio of the grains in Fig. 4c was close to Ca:Cu = 1:1. No calcium-rich area like that often encountered in pristine $CaCuO_2$ and shown in the B-region of Fig. 4b was observed. This offers further experimental evidence that high-pressure sintering improves the solubility of Ca in the $Ca_{1-x}CuO_2$ structure and this is consistent with the results of powder XRD.

Singh et al. suggested that hydrostatic pressure tends to suppress the formation of low-density, highly oxidized $Ca_{1-x}CuO_2$ and permits the insertion of a dense $CaCuO_2$ infinite layer sequence into a HTSC structure [28]. We did not find any trace of a $CaCuO_2$ infinite layer in the pressure range from 3.5 to 5 GPa using powder XRD measurements. The calcium content of $Ca_{1-x}CuO_2$ tended toward $CaCuO_2$ under higher pressures and this is a positive sign since this chemical stoichiometry would favor formation of a $CaCuO_2$ infinite layer. Transformation to the infinite-layered $CaCuO_2$ might occur at different pressures and temperatures.

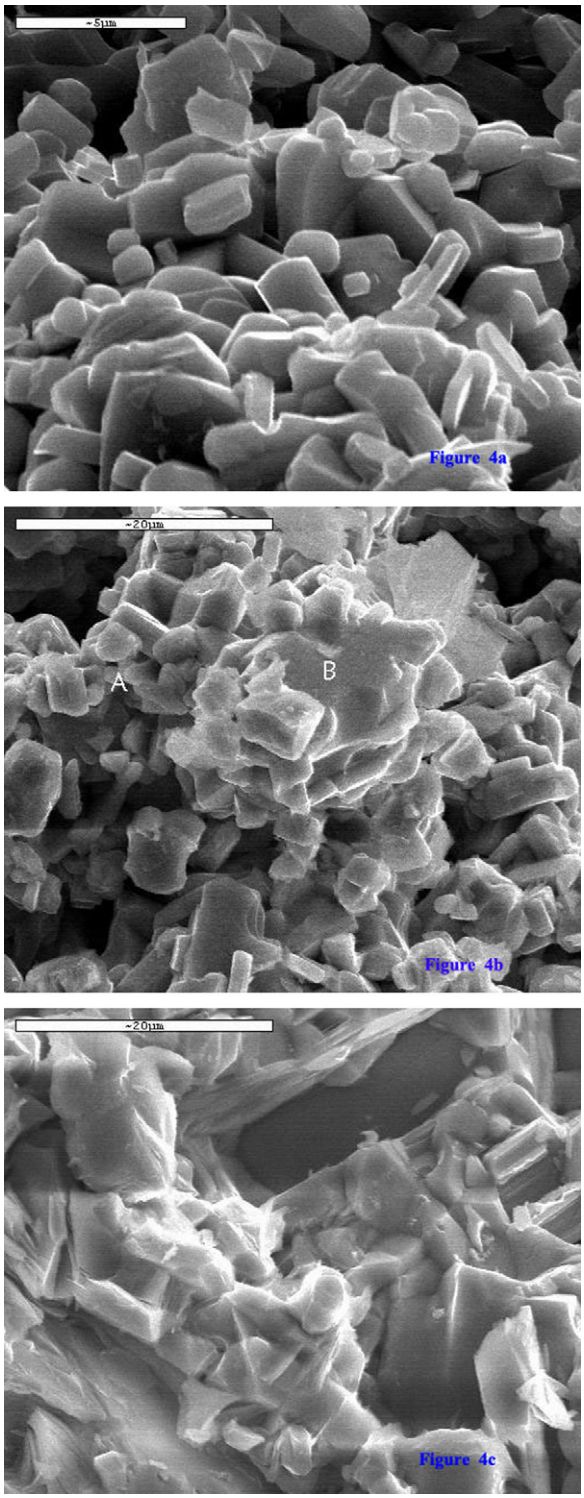

Fig. 4. (a) SEM micrograph of pristine $Ca_{0.85}CuO_2$. (b) SEM micrograph of a $CaCuO_2$ sample before high-temperature and high-pressure treatment. (c) SEM micrograph of a $CaCuO_2$ sample after high-temperature and high-pressure treatment (4 GPa, 1030 °C, 20 min).

4. Summary

$Ca_{1-x}CuO_2$ ($x = 0$, 0.15) samples were fabricated in a moderate oxygen pressure atmosphere. Through a systematic investigation, we found that the $Ca_{1-x}CuO_2$ chain structure remained stable under high temperature (≈1000 °C), high pressure (≈5 GPa) and high oxygen pressure conditions. We were thus able to study crystal doping under high pressure and also observe the resultant changes in physical properties. Interestingly, we observed that the calcium solubility rapidly increased in the $CaCuO_2$ chain structure under high pressure implying that Ca atoms might return to the vacancies of the non-stoichiometric $Ca_{1-x}CuO_2$ chain structure upon applica-

tion of high-pressure sintering. The change of Cu valency would thus be expected to induce many interesting changes in the physical properties, such as magnetism, of the $Ca_{1-x}CuO_2$ chain structure.

Acknowledgments

This work was financially supported by the Shanghai Normal University Program (SK200708), the Innovation Program of Shanghai Municipal Education Commission (09YZ151), and the Leading Academic Discipline Project (no. DZL804) of Shanghai Normal University, the Natural Science Foundation of China and the Hundred Talents Program of the Chinese Academy of Sciences.

References

[1] N. Kobayashi, Z. Hiroi, M. Takano, J. Solid State Chem. 132 (1997) 274.
[2] C.L. Teske, H. Müller-Buschbaum, Z. Anorg. Allg. Chem. 379 (1970) 234.
[3] C.L. Teske, H. Müller-Buschbaum, Z. Anorg. Allg. Chem. 370 (1969) 134.
[4] J. Karpinski, H. Schwer, I. Mangelschots, K. Conder, A. Morawski, T. Lada, A. Paszewin, Physica C 234 (1994) 10.
[5] R.S. Roth, C.J. Rawn, J.J. Ritter, B.P. Burton, J. Am. Ceram. Soc. 72 (1989) 1545.
[6] T.G.N. Babu, C. Greaves, Mater. Res. Bull. 26 (1991) 499.
[7] T. Siegrist, S.M. Zahurak, D.W. Murphy, R.S. Roth, Nature (Lond.) 334 (1988) 231.
[8] M. Uehara, T. Nagata, J. Akimitsu, H. Takahashi, N. Môri, K. Kinoshita, J. Phys. Soc. Japan 65 (1996) 2764.
[9] M. Matsukawa, Y. Yamada, M. Chibe, H. Ogasawara, T. Shibata, A. Matsushita, Y. Takano, Physica C 411 (2004) 101.
[10] C.-Q. Jin, S. Adachi, X.-J. Wu, H. Yamauchi, S. Tanaka, Physica C 223 (1994) 238.
[11] C.Q. Jin, C.J. Liu, H. Yamauchi, Phys. Rev. B 53 (1996) 5170.
[12] A. Hayashi, B. Batlogg, R.J. Cava, Phys. Rev. B 58 (1998) 2678.
[13] M.K. Wu, J.R. Ashburn, C.J. Torng, P.H. Hor, R.L. Meng, Z.J. Huang, Y.Q. Wang, C.W. Chu, Phys. Rev. Lett. 58 (1987) 908.
[14] G.M. Zhang, W.J. Mai, F.Y. Li, Z.X. Bao, R.C. Yu, J. Liu, T.Q. Lu, C.Q. Jin, Phys. Rev. B 67 (2003) 212102.
[15] T. Siegrist, R.S. Roth, C.J. Rawn, J.J. Ritter, Chem. Mater. 2 (1990) 192.
[16] M. Isobe, K. Kimoto, E. Takayama-Muromachi, J. Phys. Soc. Japan 71 (2002) 782.
[17] O. Milat, G. Van Tendeloo, S. Amelinckx, T.G.N. Babu, C. Greaves, Solid State Commum. 79 (1991) 1059.
[18] P.K. Davies, J. Solid State Chem. 95 (1991) 365.
[19] R.S. Roth, N.M. Huang, C.J. Rawn, B.P. Burton, J.J. Ritter, J. Am. Ceram. Soc. 74 (1991) 2148.
[20] J. Dolinsek, D. Arcon, P. Cevc, O. Milat, M. Miljak, I. Aviani, Phys. Rev. B 57 (1998) 7798.
[21] Z. Hiroi, M. Okumura, T. Yamada, M. Takano, J. Alloys Compd. 317 (2001) 164.
[22] F. Mezzadri, M. Calicchio, E. Gilioli, R. Cabassi, F. Bolzoni, G. Calestani, F. Bissoli, Phys. Rev. B 79 (2009) 014420.
[23] Ken Niwa, Masashi Hasegawa, Takehiko Yagi, J. Alloys Compd. 477 (2009) 493.
[24] Z.A. Ren, G.C. Che, Y.M. Ni, C. Dong, H. Chen, S.L. Jia, Z.X. Zhao, Phys. Rev. B 69 (2004) 014507.
[25] K. Kitagawa, N. Katayama, H. Gotou, T. Yagi, K. Ohgushi, T. Matsumoto, Y. Uwatoko, M. Takigawa, Phys. Rev. Lett. 103 (2009) 257002.
[26] M.G. Smith, A. Manthiram, J. Zhou, J.B. Goodenough, J.T. Markert, Nature (Lond.) 351 (1991) 549.
[27] L. Gao, Y.Y. Xue, F. Chen, Q. Xiong, R.L. Meng, D. Ramirez, C.W. Chu, Phys. Rev. B 50 (1994) 4260.
[28] K.K. Singh, D.E. Morris, A.P.B. Sinha, Physica C 231 (1994) 377.